Electromagnetics, 31:117–126, 2011
Copyright © Taylor & Francis Group, LLC
ISSN: 0272-6343 print/1532-527X online
DOI: 10.1080/02726343.2011.548193

Downloaded By: [Zhang, Wenmei] At: 23:06 28 February 2011

A Novel Differential Dual-Band Bandpass Filter Based on Stepped-Impedance Double-Sided Parallel-Strip Line

XINWEI CHEN,[1] RUNBO MA,[1] LIPING HAN,[1] GUORUI HAN,[1] LI LI,[1] and WENMEI ZHANG[1]

[1]College of Physics and Electronics Engineering, Shanxi University, Taiyuan, Shanxi, P.R. China

Abstract *A novel differential dual-band bandpass filter based on a stepped-impedance double-sided parallel-strip line is proposed in this article. In order to suppress the common-mode signal, an H-shaped ground plane is inserted. The simulated and measured results show that the proposed filter operated at 2.4 GHz and 5.8 GHz with the insertion losses of 3.2 dB and 3.5 dB, respectively. Also, the common-mode signal is suppressed to below −30 dB from 1 GHz to 7.5 GHz.*

Keywords differential, dual-band bandpass, filter, double-sided parallel-strip line, common-mode

1. Introduction

Rapid development of wireless communications presents an extraordinary demand for a differential RF front end. Differential circuits have the advantage of reducing environmental noise and improving the dynamic range of the system compared with the nondifferential circuit. A differential bandpass filter is a key component in a differential system. Recently, some single passband differential filters were proposed in Wu et al. (2007) and Shi et al. (2008). In Wu et al. (2007), a fourth-order balanced filter was proposed based on the $\lambda/2$ stepped-impedance resonators (SIRs). In Shi et al. (2008), a differential bandpass filter based on a double-sided parallel-strip line (DSPSL) dual-mode resonator was proposed. However, the dual-band bandpass filter has become a necessity in recent wireless communication systems, such as GPS, Global System for Mobile Communications (GSM), Personal Communications Service (PCS), and IMT-2000, and numerous filter designs for dual-frequency operation have been reported (Miyake et al., 1997; Lee & Hsu, 2006; Zhang & Sun, 2006; Chen et al., 2006). In Miyake et al. (1997), the transmission zeros are introduced in the middle passband of a wide bandpass filter to enforce the emergence of two separate passbands. Furthermore, some dual- and tri-band filters have been designed by using SIRs (Lee & Hsu, 2006; Zhang & Sun, 2006; Chen et al., 2006).

In this article, a novel differential dual-band bandpass filter based on a stepped-impedance DSPSL is proposed. In order to suppress the common-mode signal, an H-

Received 21 May 2010; accepted 23 August 2010.
Address correspondence to Dr. Wenmei Zhang, Shanxi University, College of Physics and Electronics, Taiyuan, Shanxi, 030006, P.R. China. E-mail: zhangwm@sxu.edu.cn

shaped ground plane is inserted. In case of differential excitation, the stepped-impedance DSPSL can be divided into two back-to-back microstrip circuits that consist of two $\lambda/4$ SIRs and two $\lambda/4$ uniform-impedance resonators (UIRs). The operation frequency can be determined by the SIRs and UIRs. Under the common-mode excitation, the H-shaped ground plane weakens the electric field between the DSPSL and the ground plane that the common-mode signal is largely suppressed. The measured results show that the proposed filter operates at 2.4 GHz and 5.8 GHz, with the high common-mode suppression better than −30 dB from 1 GHz to 7.5 GHz.

2. Structure and Theory

The proposed differential dual-band bandpass filter is shown in Figure 1(a). There are three layers of metal (a top layer, a bottom layer, and a ground plane) and two layers of substrate (substrate 1 and substrate 2). On the top and bottom layer, the SIRs and UIRs are used (Figure 1(b)). The UIR is used to strengthen the couple for the second band. The fundamental resonant frequency and the first spurious resonant frequency of the SIRs can be adjusted at two bands of a dual-band resonator and form a dual-band filter, respectively. In order to improve the common-mode suppression, the H-shaped ground plane (shown in Figure 1(c)) is inserted between substrate 1 and substrate 2. In this case, the SIRs become the stepped-impedance DSPSL. The DSPSL is connected to the ground plane through holes.

Under the differential-mode excitation, a perfect electric conductor (PEC) wall will appear on the plane between the two layers of substrate. The PEC can function as a virtual ground and overlap with the H-shaped ground plane. In this case, the stepped-impedance DSPSL can be divided into two back-to-back microstrip circuits that consist of two $\lambda/4$ SIRs and two $\lambda/4$ UIRs. The operation frequency can be determined by the SIRs and UIRs, and the design method is the same as the microstrip structure (Xinwei et al., 2009). For the proposed dual-band bandpass filter, the SIRs operate at the expected first and second frequencies (f_{d1} and f_{d2}), while the UIRs operate at the second frequency (f_{d2}).

For the $\lambda/4$ SIR, the following resonance condition is given (Sagawa et al., 1997):

$$R_z = Z_2/Z_1 = \tan\theta_1 \tan\theta_2, \tag{1}$$

where Z_1 and Z_2 are the characteristic impedance of a wide microstrip line and a narrow microstrip line of the SIR, θ_1 and θ_2 are their electrical lengths, and R_z is the impedance ratio. According to Eq. (1), the R_z and $U = \theta_2/(\theta_1 + \theta_2)$ can be selected under the conditions of f_{d1} and f_{d2}.

Under common-mode excitation, a perfect magnetic conductor (PMC) wall will appear on the ground plane. The impact of the H-shaped ground on the common-mode suppression can be seen in Figure 2. It indicates, in the case of $w_{g1} = 9$ mm, that the whole ground has the same shape with the substrate. In this case, the electronic field will be formed between the top (or bottom) layer and ground, so the common-mode signal can be transmitted from the input port to the output port. As w_{g1} is reduced, the electronic field will be disturbed; thus, the transmission of the common-mode signal is weakened. When $w_{g1} = 3$ mm, most of the electronic field is destroyed; the potential distribution on the top and bottom layer is the same, and almost no electric field can be formed between those for which the common-mode signal is largely suppressed. Finally, in order to guarantee feeding for the microstrip line and connect the ground via holes, an H-shaped ground plane is selected.

Downloaded By: [Zhang, Wenmei] At: 23:06 28 February 2011

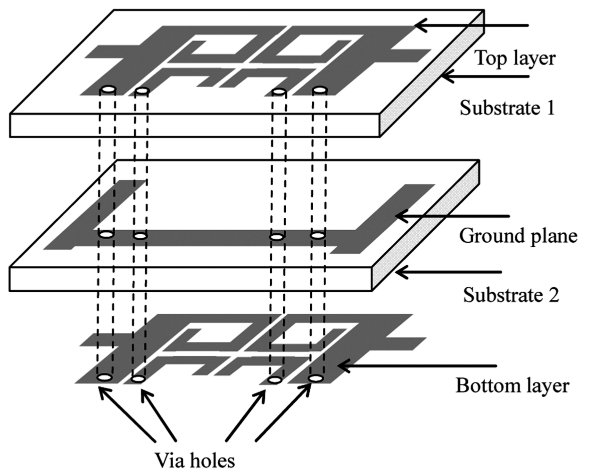

(a)

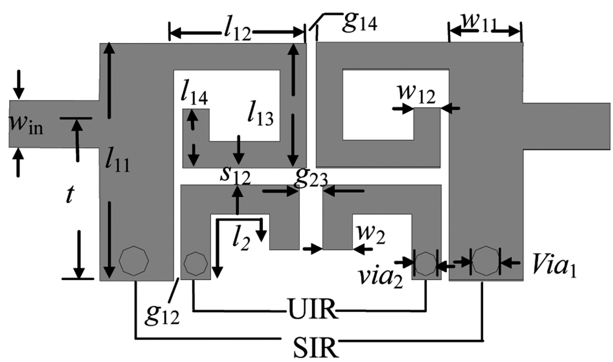

(b)

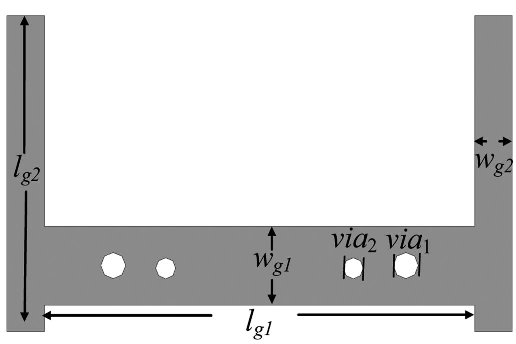

(c)

Figure 1. The proposed differential dual-band bandpass filter: (a) configuration of the filter, (b) top layer structure, and (c) H-shaped ground.

Downloaded By: [Zhang, Wenmei] At: 23:06 28 February 2011

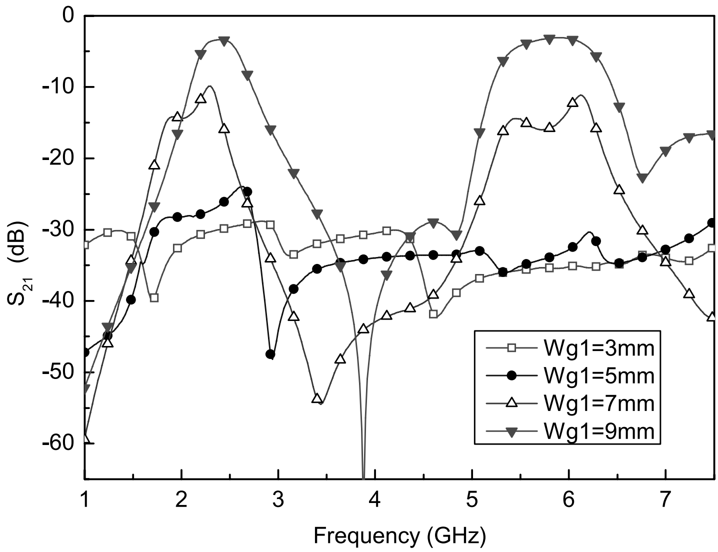

Figure 2. The common-mode response for different H-shaped grounds.

Downloaded By: [Zhang, Wenmei] At: 23:06 28 February 2011

The operation of the proposed filter can be described by the surface current distribution, as shown in Figure 3. Figures 3(a) and 3(b) show the differential-mode surface current distribution at 2.4 GHz and 5.8 GHz. It is shown that the signal is coupled through SIRs directly at 2.4 GHz, while at 5.8 GHz, the signal is coupled through UIRs and SIRs. Figures 3(c) and 3(d) show the common-mode surface current distribution at 2.4 GHz and 5.8 GHz. It can be seen that a current circuit appears between the top layer circuit and the H-shaped ground; however, no current is coupled to the output at 2.4 GHz and 5.8 GHz.

3. Design and Results

As a demonstration example, a dual-band bandpass filter is designed and fabricated with the following specifications:

$f_{d1} = 2.4$ GHz,
$f_{d2} = 5.8$ GHz,
$FBW_1 = FBW_2 = 15\%$,
$S_{21} < -30$ dB for the common mode.

where FBW = fractional bandwidth.

According to the design specifications, the butterworth and quasi-elliptic low-pass prototype are selected at f_{d1} and f_{d2}, respectively.

The two circuits of the top and bottom layers are designed to realize the differential-mode response. It operates at 2.4 GHz and 5.8 GHz; hence, $Rz = 2$ and $U = 0.6$ are chosen. Meanwhile, the UIR resonates at 5.8 GHz.

The other design parameters of the circuits of the top and bottom layers, i.e., the coupling coefficients and external quality factor, can be obtained from circuit elements of a low-pass prototype filter, which are listed in Table 1 (Jia & Lancaster, 2001).

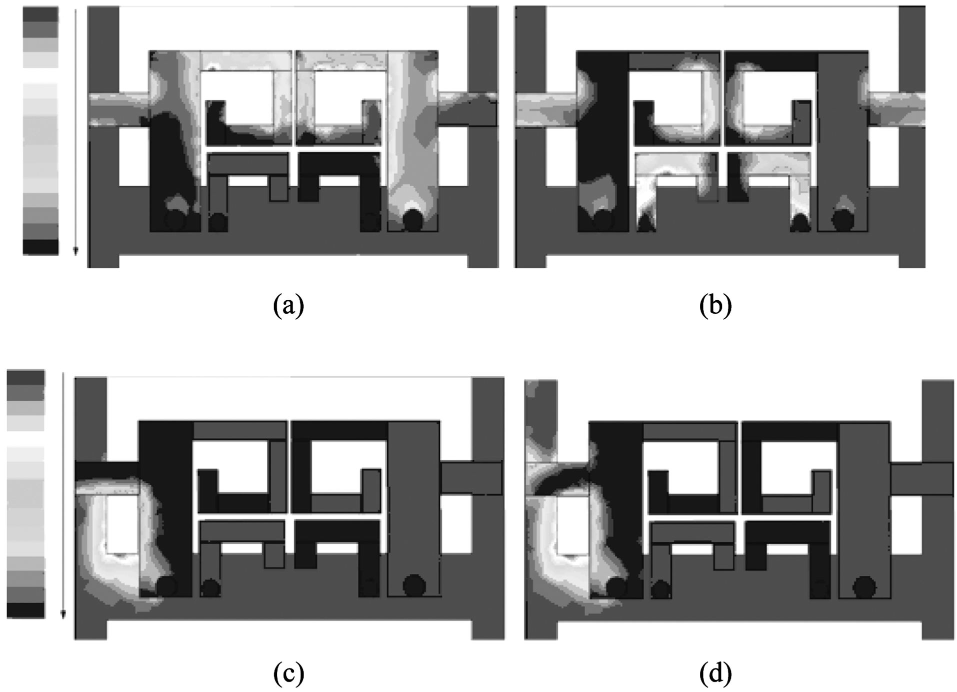

Figure 3. The surface current distribution of proposed filter at: (a) 2.4 GHz for differential-mode excitation, (b) 5.8 GHz for differential-mode excitation, (c) 2.4 GHz for common-mode excitation, and (d) 5.8 GHz for common-mode excitation.

The full-wave simulator has been used to extract the above parameters. Figure 4 shows the differential-mode external quality factors versus the tap position of I/O resonators. Figure 5 shows the differential-mode coupling coefficients versus the gaps between adjacent resonators. The required physical parameters are then obtained from Figures 4 and 5.

The filter is fabricated on a FR4 substrate ($\varepsilon_r = 4.4$, $h = 0.8$ mm, $\tan\delta = 0.02$). The simulations are carried out using Ansoft designer (SV; ANSYS Inc., Canonsburg, Pennsylvania, USA). The optimized parameters are $l_{11} = 8$ mm, $l_{12} = 4.5$ mm, $l_{13} =$

Table 1
Design parameters of filter

Center band	Element values of low-pass prototype	Design parameters
First passband	$g_0 = g_3 = 1$, $g_1 = g_2 = 1.4142$	$M_{14} = 0.11$, $Q_{ei} = Q_{eo} = 9.43$
Second passband	$g_1 = 0.95691$, $g_2 = 1.39927$, $J_1 = -0.18429$, $J_2 = 1.08548$	$M_{12} = M_{34} = 0.129$, $M_{23} = 0.116$, $M_{14} = -0.028$, $Q_{ei} = Q_{eo} = 6.38$

Downloaded By: [Zhang, Wenmei] At: 23:06 28 February 2011

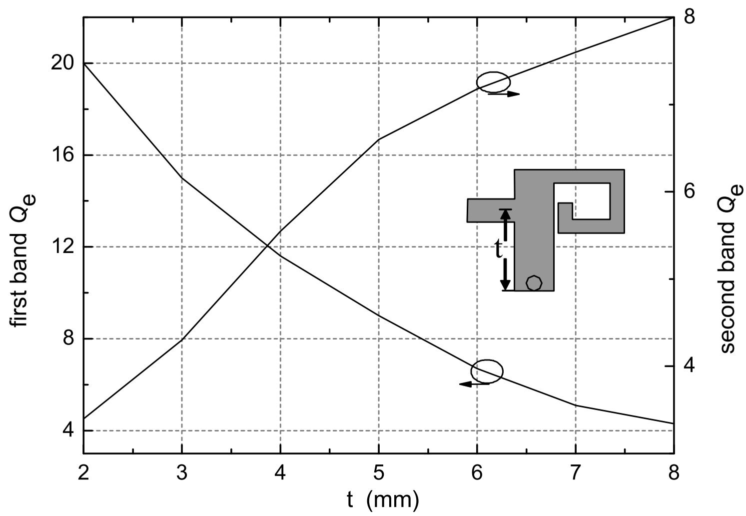

Figure 4. Differential-mode external quality factors versus the tap position of I/O resonators.

3.3 mm, $l_{14} = 2$ mm, $w_{11} = 2.5$ mm, $w_{12} = 0.9$ mm, $l_2 = 7.8$ mm, $w_2 = 1$ mm, $w_{in} = 1.5$ mm, $g_{12} = 0.2$ mm, $s_{12} = 0.4$ mm, $g_{23} = 0.54$ mm, $g_{14} = 0.33$ mm, $t =$ 5 mm, $via_1 = 0.5$ mm, $via_2 = 0.4$ mm, $l_{g1} = 17.2$ mm, $l_{g2} = 12$ mm, $w_{g1} = 3$ mm, $w_{g2} = 1.5$ mm. The photograph of the proposed filter is shown in Figure 6.

The standard four-port S-parameters are measured with the Agilent N5230A vector network analyzer (Agilent Technologies Inc., Morgan Hill, California, USA). The two-

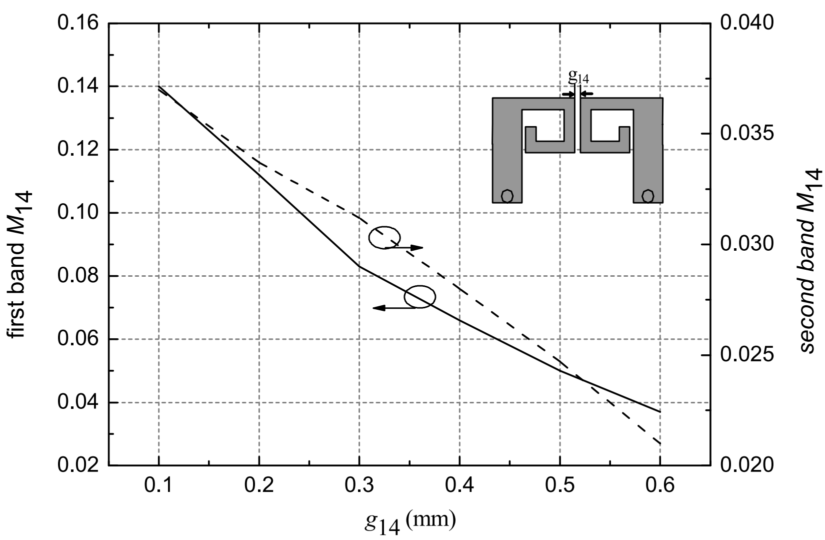

(a)

Figure 5. Differential-mode coupling coefficients versus the gaps between adjacent resonators: (a) magnetic coupling, (b) electric coupling, and (c) mixed coupling. (*continued*)

Downloaded By: [Zhang, Wenmei] At: 23:06 28 February 2011

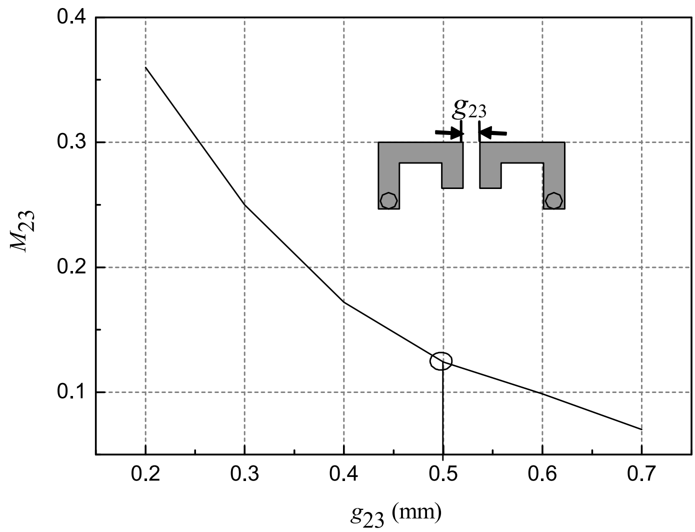

(b)

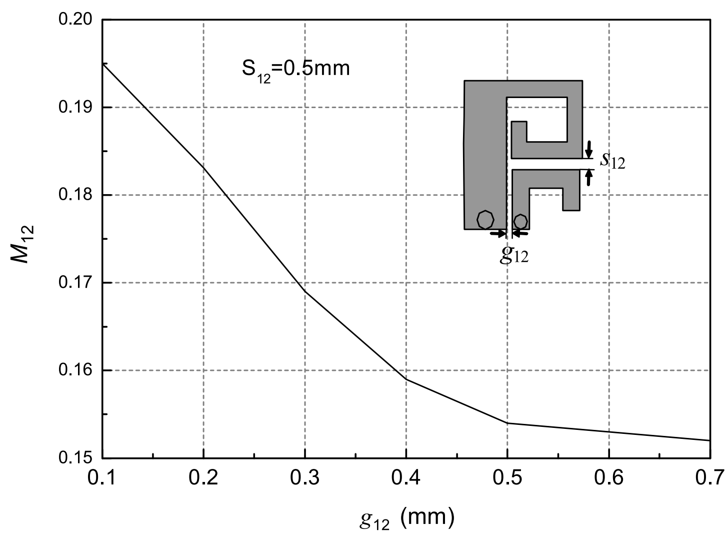

(c)

Figure 5. (*Continued*).

Downloaded By: [Zhang, Wenmei] At: 23:06 28 February 2011

port differential-mode and common-mode S-parameters can be extracted from standard four-port S-parameters as given in Bockelman and Eisenstant (1995). The simulated and measured differential-mode and common-mode responses of the designed filter are shown in Figures 7 and 8. Figure 7 shows the differential-mode response. It indicates that the first passband is at 2.4 GHz with an insertion loss of less than 3.2 dB and 3-dB FBW of 12.4%, and the second passband is at 5.8 GHz with an insertion loss of less than 3.5 dB and 3-dB FBW of 15%. Figure 8 shows the common-mode response of the

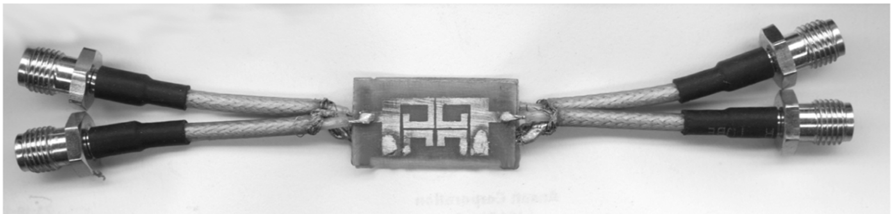

(a)

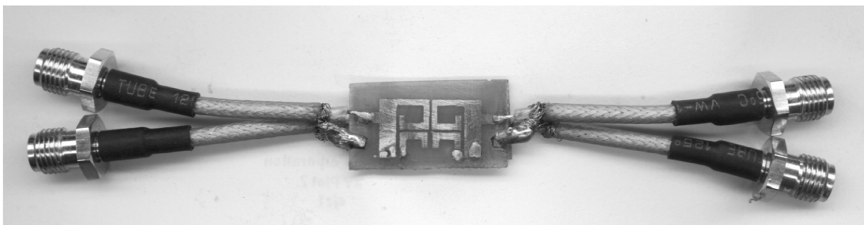

(b)

Figure 6. Photograph of the proposed filter: (a) top view and (b) bottom view.

Downloaded By: [Zhang, Wenmei] At: 23:06 28 February 2011

proposed filter. It can be seen that the common-mode signal is suppressed with the level of −34 dB and −41 dB at 2.4 GHz and 5.8 GHz, respectively. Moreover, common-mode signal is suppressed below −30 dB from 1 GHz to 7.5 GHz. Compared with the simulated results, the passbands are narrowed and the attenuation poles shift slightly. The changes are mainly caused by the fabrication error of the line spacing and the electric constant deviation of the fabricated FR4.

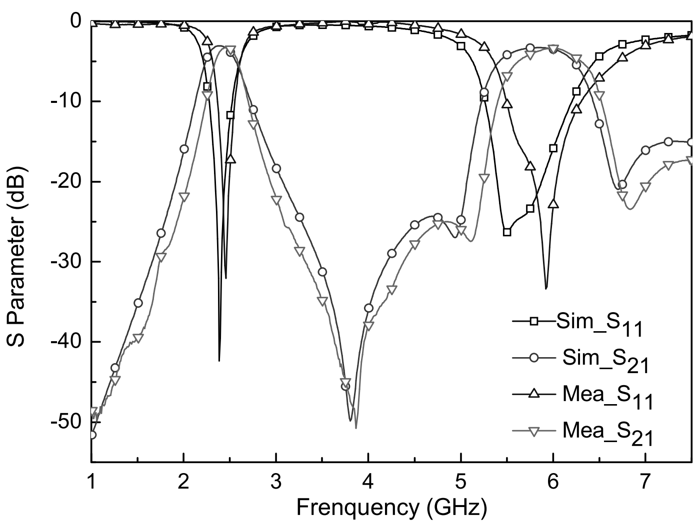

Figure 7. Differential-mode response.

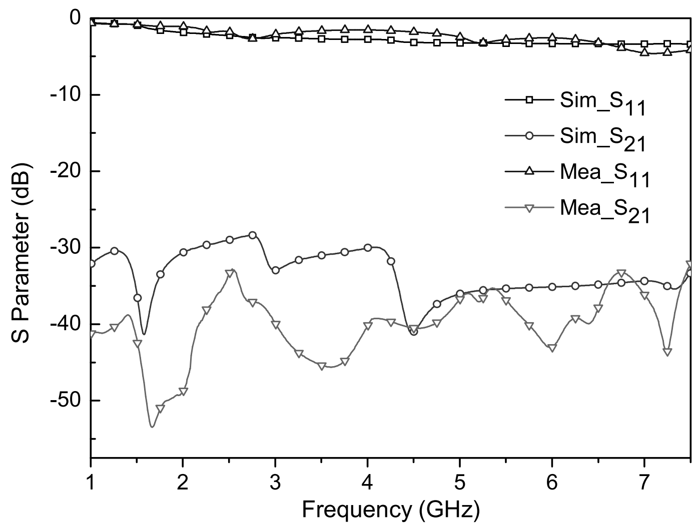

Figure 8. Common-mode response.

Downloaded By: [Zhang, Wenmei] At: 23:06 28 February 2011

4. Conclusions

A novel differential dual-band bandpass filter based on a stepped-impedance DSPSL is proposed in this article. The higher common-mode suppression is obtained by inserting an H-shaped partial ground plane. Simulated and measured results indicate that it is better than −30 dB from 1 GHz to 7.5 GHz.

Acknowledgments

This work was supported by the National Science Foundation of China (no. 60771052), the Special Item of China Postdoctor Science Foundation (200801424), the Natural Science Foundation of Shanxi province (nos. 2006011029, 2010021015-1), and the Program for the Top Young Academic Leaders of Higher Learning Institutions of Shanxi.

References

Bockelman, D. E., &, W. R. Eisenstant. 1995. Combined differential and common-mode scattering parameters: Theory and simulation. *IEEE Trans. Microw. Theory Techniq.* 43:1530–1539.

Chen, C. F., T. Y. Huang, & R. B. Wu. 2006. Design of dual- and triple-passband filters using alternately cascaded multiband resonators. *IEEE Trans. Microw. Theory Techniq.* 54:3550–3558.

Jia S. H., & M. J. Lancaster. 2001. *Microstrip filters for RF/microwave applications*. New York: Wiley.

Lee, C. H. & C. I. G. Hsu. 2006. Design of a new tri-band microstrip BPF using combined quarter-wavelength SIRs. *IEEE Microw. Wireless Compon. Lett.* 16:594–596.

Miyake, H., S. Kitazawa, T. Ishizaki, T. Yamada, & Y. Nagatomi. 1997. A miniaturized monolithic dual bands filter using ceramic lamination technique for dual mode portable telephones. *Microw. Symp. Digest 1997 (IEEE MTT-S Intl.)* 2:789–792.

Sagawa, M., M. Makimoto, & S. Yamashita. 1997. Geometrical structures and fundamental characteristics of microwave stepped-impedance resonators. *IEEE Trans. Microw. Theory Techniq.* 45:1078–1084.

Shi, J., J. X. Chen, & Q. Xue. 2008. A novel differential bandpass filter based on double-side parallel-strip line dual-mode. *Microw. Optical Technol. Lett.* 50:1733–1735.

Wu, C.-H., C.-H. Wang, & C. H. Chen. 2007. Stopband-extended balanced bandpass filter using coupled stepped-impedance resonators. *IEEE Microw. Wireless Compon. Lett.* 17:507–509.

Xinwei, C., H. Guorui, M. Runbo, G. Jiangrui, & Z. Wenmei. 2009. Design of balanced dual-band bandpass filter with self-feedback structure. *ETRI J.* 31:475–477.

Zhang, Y. P., & M. Sun. 2006. Dual-band microstrip bandpass filter using stepped impedance resonators with new coupling schemes. *IEEE Trans. Microw. Theory Techniq.* 54:3779–3785.

Downloaded By: [Zhang, Wenmei] At: 23:06 28 February 2011